Chapter 7

LEARNING MECHANISMS IN NETWORKS OF SPIKING NEURONS

QingXiang Wu[12], Martin McGinnity[1], Liam Maguire[1],
Brendan Glackin[1], Ammar Belatreche[1]

[1]*School of Computing and Intelligent Systems,University of Ulster, Magee Camlus, Derry, BT48 7JL, N. Ireland, UK;* [2]*School of Physics and OptoElectronics Technology, Fujian Normal University, Fuzhou, 350007 China.*

Abstract   In spiking neural networks, signals are transferred by action potentials. The information is encoded in the patterns of neuron activities or spikes. These features create significant differences between spiking neural networks and classical neural networks. Since spiking neural networks are based on spiking neuron models that are very close to the biological neuron model, many of the principles found in biological neuroscience can be used in the networks. In this chapter, a number of learning mechanisms for spiking neural networks are introduced. The learning mechanisms can be applied to explain the behaviours of networks in the brain, and also can be applied to artificial intelligent systems to process complex information represented by biological stimuli.

Keywords: spiking neural networks, learning; spiking neuron models, spike timing-dependent plasticity, neuron encoding, co-ordinate transformation.

1.   Introduction

The first generation of neural networks is based on the model of McCulloch-Pitts neurons, as computational units in which the perceptrons are regard as threshold-gates. A characteristic feature is that such systems have digital output for every unit. For example, multiplayer perceptrons, Hopfied nets, and Boltzmann machines are based on this model. The second generation is based on computational units in which an "activation function" with a continuous set of possible output values

is applied to a weighted sum of the inputs. Common activation functions are sigmoid functions and linear saturated functions. The piecewise polynomial functions and piecewise exponential functions are also considered as activation functions, for example feed forward and recurrent neural networks, and radial basis networks. These networks can compute certain Boolean functions with fewer gates than first generation networks [1], and are able to compute functions with analog input and output. These two generations of neural networks focus on a small number of aspects of biological neurons. The third generation [2] of neural networks is based on the Hodgkin-Huxley spiking neuron model [3], [4]. The functionalities of the spiking neurons can be applied to deal with biological stimuli and explain complicated intelligent behaviours of the brain. A distinct feature of spiking neural networks is that significant information is encoded in the neural activity patterns and the neurons communicated using spike trains [5], [6] instead of single values, as used in the first two-generations of neural networks. Spiking neural networks always work with a large population of neurons. As a large-scale network of spiking neurons requires high computational resources to simulate, the integrate-and-fire neuron model and spike response model [4] are usually regarded as a simplified Hodgkin-Huxley model. Since spiking neuron models are employed and information is encoded using the patterns of neural activities, learning mechanisms for spiking neural networks are very different from that in the first two-generations of classical neural networks. Initially, researchers tried to apply traditional learning mechanisms to spiking neural networks. SpikeProp [7], which is similar to the classical BP algorithm, has been proposed to train spiking neural networks. The neuron model employed in the SpikeProp network is based on a spike response model and assumes that each neuron only fires once during a period. This work proves that networks of spiking neurons are able to be trained to perform classification and function approximation. Using parallel calculations, the network can be trained by fewer epochs than a classical neural networks for the same classification problem [7], [8]. Based on a spike response neuron model with delay encoding, a spiking neural network [9] is applied to a time-series prediction problem-laser amplitude fluctuation. In the spiking neural network, a delay is defined as the time difference between the presynaptic firing time and the time when the postsynaptic potential starts rising. Learning is the process of modifying the delay according to the time difference between presynaptic neuron firing time and the postsynaptic neuron firing time, so that the input time structure is memorized into the delay. In [10], a model of a network of integrate-and-fire neurons with time delay weights is presented. The model consists of one layer of multiple leaky

integrate-and-fire neurons fully connected with a set of temporal inputs. These inputs simulate spatiotemporal patterns formed in the olfactory bulb, and the neural layer corresponds to the olfactory cortex that receives and recognizes those patterns. The periodic inputs are expressed by a Dirac delta function. The phase shifts of the input spikes encode concentrations of the corresponding constituent molecules. The total time delay of an input signal that arrives at an output neuron is equal to the sum of the phase shift and the additional time delays stored in the synaptic connections. The Hopfield's phase shift encoding principle at the output level is applied for spatiotemporal pattern recognition. Firing of an output neuron indicates that corresponding odour is recognized and phase shift of its firing encodes the concentration of the recognized odour. The learning mechanism is to update the delays and weights [10]. The result shows that the approach is capable of invariant spatiotemporal pattern recognition. The temporal structure of the model provides the base for the modeling of higher-level tasks, where temporal correlation is involved, such as feature binding and segmentation, object recognition, etc.

The networks of spiking neurons are capable of self-organization in different ways. A model of this type of network was applied in the pattern interaction and orientation maps in the primary visual cortex [11], [12]. Spiking neurons with leaky integrator synapses were used to model image segmentation and binding by synchronization and desynchronization of neuronal group activity. The advantage is that the network can model self-organization and functional dynamics of the visual cortex at a more accurate level than earlier models.

Since spiking neuron models are very close to biological neurons, many findings in neuroscience can be simulated using spiking neural networks. Based on spike timing dependent plasticity (STDP) found in biological neurons [13], [14], [15], [16], a set of learning mechanisms are demonstrated in this chapter.

2.   Spiking Neuron Models

2.1   Hodgkin-Huxley Spiking Neuron Model

Hodgkin and Huxley [3] performed experiments on the giant axon of the squid and found three different types of ion current. The equations of Hodgkin and Huxley describe the electro-physiological properties of the giant axon of the squid. The basic mechanism of generating action potentials or spikes is a short influx of sodium ions that is followed by
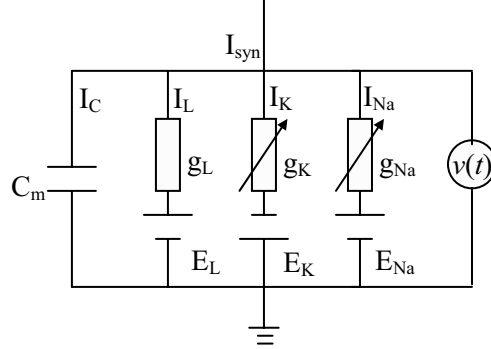
Figure 7.1. Equivalent circuit for the Hodgkin-Huxley neuron model

an efflux of potassium ions. Let v represent the membrane potential of a neuron. The basic equation of spiking neuron models is given by

$$c_m \frac{dv(t)}{dt} = I_C = I_{syn}(t) - \sum_j I_j(t) \qquad (7.1)$$

where C_m is the membrane capacity, I_{syn} the synaptic input current, and I_j is the current through ion channel j. Three types of channels can be regarded as an equivalent circuit in Fig. 7.1. The Hodgkin-Huxley model describes three types of channels. All channels may be characterized by their resistance or, equivalently, by their conductance. The leakage channel is described by a voltage-independent conductance g_L; the conductance of the other ion channels is voltage and time dependent. If all channels are open, they transmit currents with a maximum conductance g_{Na} or g_K, respectively. Normally, some of the channels are blocked. The probability that a channel is open is described by additional variables m, n, and h. The combined action of m and h controls the Na$^+$ channels. The K$^+$ gates are controlled by n. Specifically, Hodgkin and Huxley formulated the three current components as

$$\sum_j I_j = g_{Na}m^3h(v(t) - E_{Na}) + g_K n^4(v(t) - E_K) + g_L(v(t) - E_L) \quad (7.2)$$

The parameters E_{Na}, E_K, and E_L are the reversal potentials. Reversal potentials and conductance are empirical parameters from biological neurons. For example, a set of typical parameters are shown as follows.
$E_{Na} = 50$mV; $E_K = -77$mV; $E_L = -54.4$mV; $g_{Na} = 120$mS/cm^2; $g_K = 36$mS/cm^2; $g_L = 0.3$ms/cm^2. Three gating variables are expressed

Table 7.1.   Parameters for channel control equations

x	$\alpha_x(v)$	$\beta_x(v)$
m	$(0.1v + 8.5)/[\exp(0.1v + 8.5) - 1]$	$4\exp[(65 - v)/18]$
n	$(0.75 - 0.01v)/[\exp(7.5 - 0.1v) - 1]$	$0.125\exp[(65 - v)/80]$
h	$0.07\exp[(65 - v)/20]$	$1/[\exp(9.5 - 0.1v) + 1]$

by the following differential equations.

$$\begin{aligned} \dot{m} &= \alpha_m(v)(1 - m) - \beta_m(v)m \\ \dot{n} &= \alpha_n(v)(1 - n) - \beta_n(v)n \\ \dot{h} &= \alpha_h(v)(1 - h) - \beta_h(v)h \end{aligned} \tag{7.3}$$

Where $\alpha_x(v)$ and $\beta_x(v)$ for $x \in \{m, n, h\}$ are dependent on membrane potential v. The relationships are shown in Table 7.1.

The single neuron model was implemented in the NEURON spiking neural network simulation package [17]. The synapse current is not always a constant. Different synapse models were used to model synapse current such as a square pulse, exponential pulse, alpha function, etc.

2.2   Integrate-and-Fire Neuron Model

As mentioned in Section 2.1, the Hodgkin-Huxley spiking neuron is governed by differential equations (7.1), (7.2), and (7.3). If this model is applied to a large scale network, the implementation will encounter a very high computational complexity. Therefore, a set of simplified models were proposed. For example, the NEURON software provides three types of integrated-and-fire neuron models, i.e. IntFire1, IntFire2 and IntFire4 [17], [41]. A spiking response model with temporal encoding was used in [7], [18]. In this chapter, the conductance-based integrate-and-fire model is used for each neuron in SNNs because the behaviour of this neuron model is very close to the Hodgkin-Huxley model [19]. In the model, the membrane potential $v(t)$ is governed by the following equations [4], [19], [20], [21].

$$c_m \frac{dv(t)}{dt} = g_l(E_l - v(t)) + \sum_j \frac{w^j g_s^j(t)}{A_s}(E_s - v(t)) \tag{7.4}$$

where c_m is the specific membrane capacitance, E_l is the membrane reversal potential, E_s is the reversal potential ($s \in \{i, e\}$, i and e indicate inhibitory and excitatory synapses respectively), w^j is a weight for synapse j, and A_s is the membrane surface area connected to a synapse. If the membrane potential v exceeds the threshold voltage v_{th}, v is reset
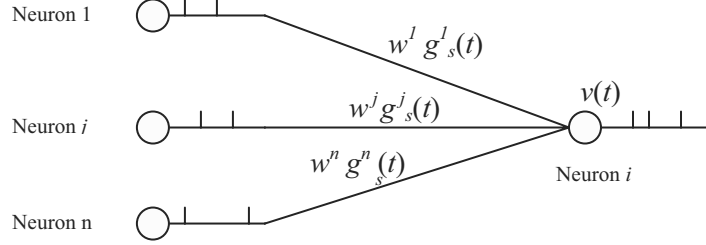
Figure 7.2.   Conductance based synapses in a SNN

to v_{reset} for a time τ_{ref} and an action potential is generated. Fig. 7.2 shows that a neuron receives spike trains from three afferent neurons in a receptive field.

The variable $g_s^j(t)$ is the conductance of synapse j. When an action potential reaches the synapse at t_{ap}, the conductance is increased by the following expression.

$$g_s^j(t_{ap} + t_{delay}^j + dt) = g_s^j(t_{ap} + t_{delay}^j) + q_s \qquad (7.5)$$

Otherwise, the conductance decays as illustrated in the following equation.

$$\frac{d\,g_s^j(t)}{dt} = -\frac{1}{\tau_s} g_s^j(t) \qquad (7.6)$$

where q_s is the peak conductance. Neuron i integrates the currents from afferent synapses and increases the membrane potential according to Equation (7.4). In this simulation, the parameters are set as follows. $t_{delay}^j = 0.$ $v_{th} = -54\,\text{mv}.$ $v_{reset} = -70\,\text{mv}.$ $Ee = 0\,\text{mv}.$ $Ei = -75\,\text{mv}.$ $q_{e\_max} = 0.01\,\mu\text{s}.$ $q_{i\_max} = 0.01\,\mu\text{s}.$ $q_e = 0.002\,\mu\text{s}.$ $q_i = 0.002\,\mu\text{s}.$ $El = -70\,\text{mv}.$ $g_l = 1.0\,\mu\text{s/mm}^2.$ $c_m = 10\,\text{nF/mm}^2.$ $\tau_e = 3\,\text{ms}.$ $\tau_i = 10\,\text{ms}.$ $A_e = 0.028953\,\text{mm}^2.$ $A_i = 0.014103\,\text{mm}^2.$

In order to show action potential or spikes generated by a single Integrate-and-Fire (I&F) neuron, 50 excitatory synapses are connected to the neuron. The mean frequency of 50 random spike trains is increasing slowly from 0 to 100 Hz. The output spikes of the spiking neuron changes from non-firing to firing at a fixed frequency. The neuron passed through three stages, as shown in Fig. 7.3. When the input spike trains are at a low firing frequency, the neuron do not fire (see Fig. 7.3(a)). The membrane potential of the neuron varies under a threshold. When the input spike trains are strong enough, the neuron enters into an irregular firing state (Fig. 7.3(b)). When the input spike trains are very strong, the neuron fires at a fixed frequency (Fig. 7.3(c)). This frequency depends on the refractory time τ_{ref} of the neuron. This is a simplest example

(a) Non-firing   (b) Irregular-firing   (c) Firing at a fixed frequency
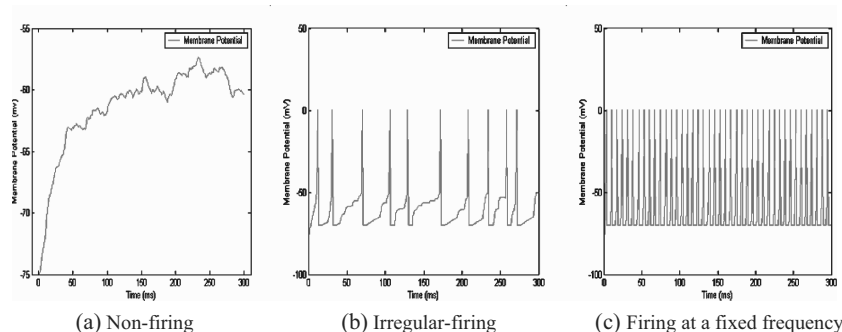
Figure 7.3.   I&F neuron response to spike trains with different frequenices
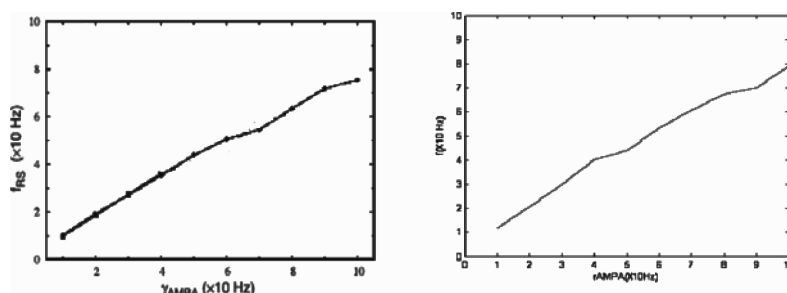

Figure 7.4.   Firing properties of a single neuron bombarded by random synaptic inputs.   Both neurons were bombarded by Poisson-distributed random synaptic (AMPA) inputs different firing rates (10Hz –100Hz), with maximal conductance of 100 nS.

for spike generation for an integrate-and-fire neuron. This conductance-based I&F neuron model is very close to the Hodgkin-Huxley-model in the NEURON software. The simulation results for both models are illustrated in Fig. 7.4. and this comparison was performed in the SenseMaker project [22].

3.   Information Encoding in SNN

Although a neuron transfers information to another neuron by means of a complicated biological process, experiments show that the action potentials or spikes [3] are the key signals. Spiking neural networks in the brain are very complicated. Thousands of spike trains are emitted constantly by different neurons. How to understand such a spatiotemporal pattern of spikes is an extremely important topic in spiking neural networks. Therefore, a wide range of different encoding schemes have been discussed in the domain of neural coding [4], [6]. For example,
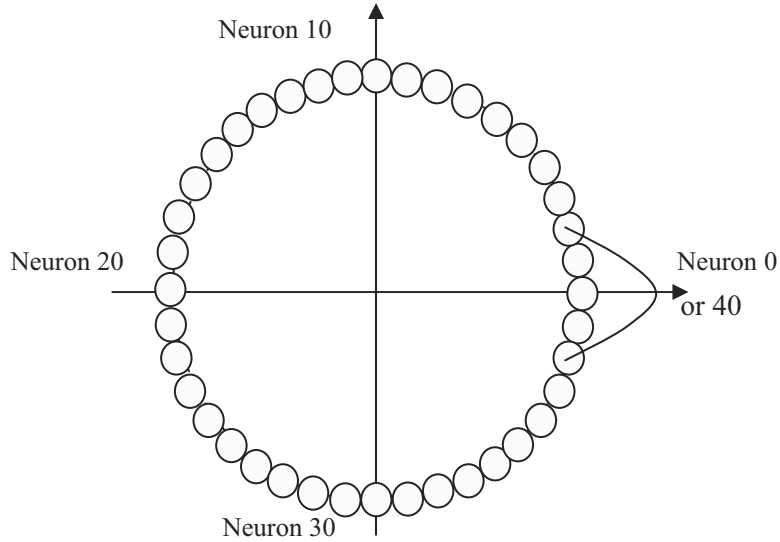
Figure 7.5. Angular variable can be represented by a circle of neuron chain

count code, binary code, timing code and rank order code were de-
scribed in [6]. Firing frequency and firing rate were described in [4].
The differences between rate encoding scheme and temporal encoding
scheme was discussed in [6]. Here, a specific spatiotemporal encoding
scheme is used. Let a circle of chain neurons shown in Fig. 7.5 represent
an angular variable. If Neuron No.0 or No.40 fires at the highest firing
rate and firing rates for neurons from No.38 to No.2 draws a bell-shaped
distribution, this pattern of the neuron activity indicates 0°. Suppose
that after 200ms the centre of the pattern moves to Neuron 1. The cor-
responding angle is $360°/40 = 9°$. By analogy, the centre of the pattern
moves from Neuron 2 to 39 step by step with step duration 200ms. The
corresponding angle can be represented by the equation $\Phi_d(t) = 9t/200$
degree, where the unit of t is ms. If the angle is represented by the centre
neuron number in the bell-shaped distribution of firing rates, the equa-
tion is written as $\Phi(t) = t/200$, where $\Phi(t)$ unit is the neuron number.
Recording all the activities of the neuron chain for 8000ms, a firing rate
raster is plotted in Fig. 7.6. Similarly, variable x can be represented by
a neuron chain. The firing pattern for $x(t) = 20 - 10\,\text{COS}(2\pi t/3600)$
is shown in Fig. 7.7. The phase encoding scheme is also used in this
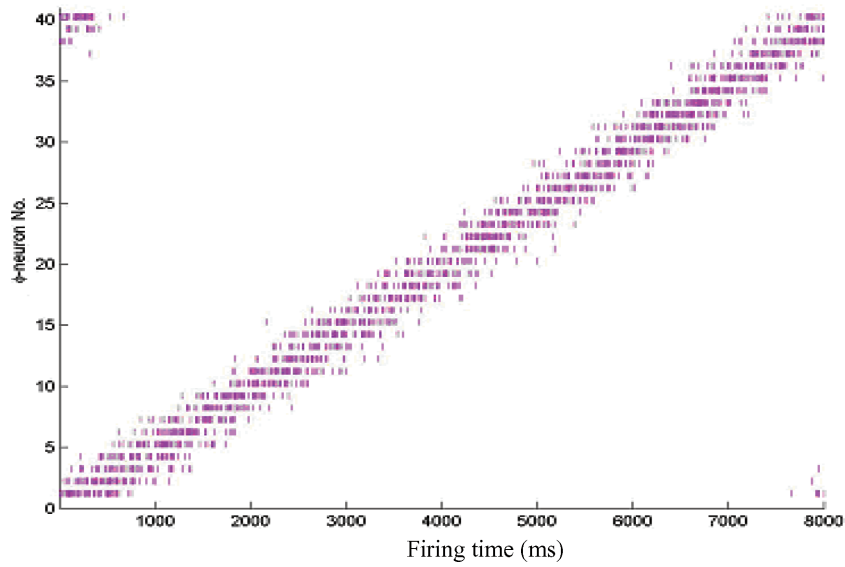chapter. Details will be given in Section 5.

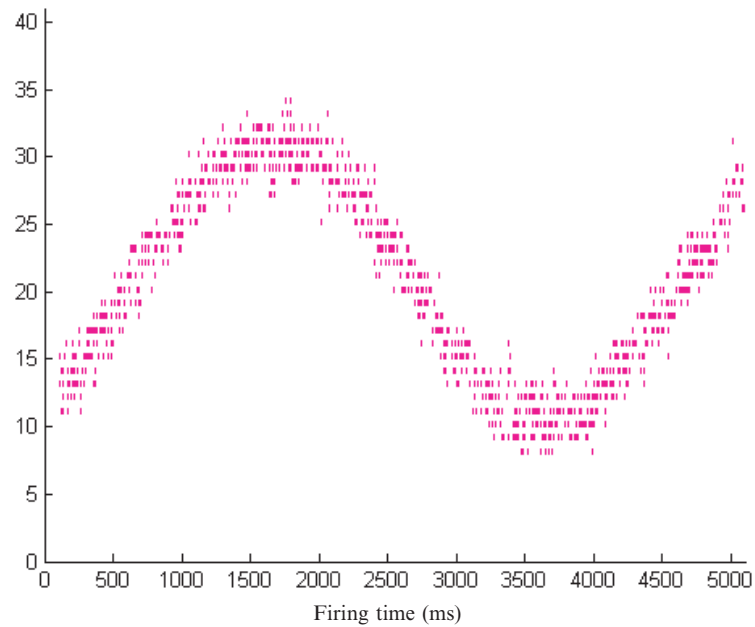*Figure 7.6.*   The firing pattern changes of neuron chain represents $\Phi(t) = t/200$ms

Figure 7.7.   The firing pattern record for $x(t) = 20 - 10 \cos(\ 2\pi t/3600)$

4.   STDP Implementation

Changes in the synaptic connections between neurons are widely believed to contribute to memory storage. These changes are thought to occur through correlation-based, Hebbian plasticity [16]. Spike Timing-Dependent Plasticity (STDP) was found in biological neurons. The synaptic plasticity model has been explored based on the fact that a synaptic potentiation and depression can be induced by precisely timed pairs of synaptic events and postsynaptic spikes [13], [14], [15].

In order to perform STDP learning in SNNs, the implementation approach in [23], [24] is applied. Each synapse in an SNN is characterized by a peak conductance q_s (the peak value of the synaptic conductance following a single presynaptic action potential) that is constrained to lie between 0 and a maximum value q_{s_max}. Every pair of pre- and postsynaptic spikes can potentially modify the value of q_s, and the changes due to each spike pair are continually summed to determine how q_s changes over time. The simplifying assumption is that the modifications are produced by linear combination of individual spike pairs.

A presynaptic spike occurring at time t_{pre} and a postsynaptic spike at time t_{post} modify the corresponding synaptic conductance by

$$q_s \leftarrow q_s + q_{s\_\max}F(\Delta t) \qquad (7.7)$$

where $\Delta t = t_{post} - t_{pre}$ and

$$F(\Delta t) = \begin{cases} A_+ \exp(\Delta t/\tau_+), & if\ \Delta t > 0 \\ -A_- \exp(\Delta t/\tau_-), & if\ \Delta t \leq 0 \end{cases} \qquad (7.8)$$

The time constants τ_+ and τ_- determine the ranges of pre- to postsynaptic spike intervals over which synaptic strengthening and weakening are significant, and A_+ and A_- determine the maximum amount of synaptic modification in each case. The function $F(\Delta t)$ for synaptic modification is shown in Fig. 7.8.

The experimental results indicate a value of τ_+ in the range of tens of milliseconds (about 20 ms). The parameters for STDP are set as follows. $q_{s\_max} = 0.01,\ A_+ = 0.01,\ A_- = 0.005,\ \tau_+ = 20\,\text{ms},\ \tau_- = 100\,\text{ms}$.

4.1   Connection Selectivity of Two-layer Network Simulations

Based on the implementation approaches[23], [24], a two layer spiking neural network with STDP connections is designed. The architecture is shown in Fig. 7.9.

The first layer consists of sensory neurons that transform stimulus strength to phase encoding and output fixed frequency spike trains.
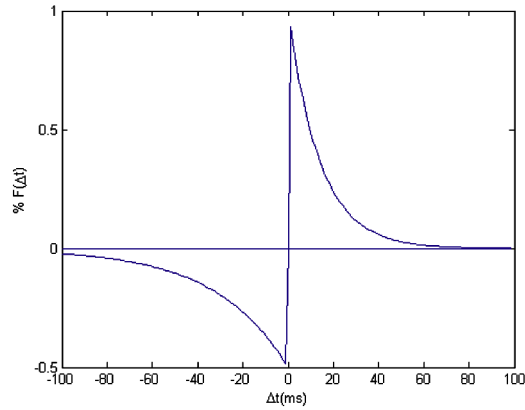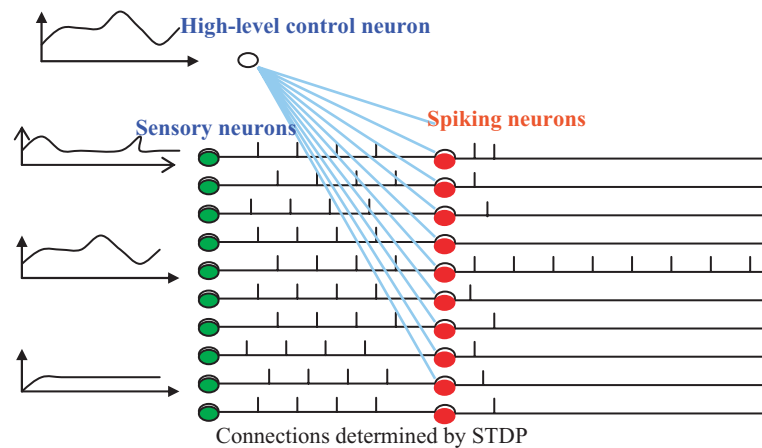
Figure 7.8. Synaptic modification

Figure 7.9. The architecture of two-layer network

The second layer contains spiking neurons that are connected to the first layer by a one-to-one configuration; the efficacy of these connections are determined by STDP learning. A high-level control neuron is fully connected to the second layer. Suppose that three different stimuli are presented to the neurons in first layer. One of the stimuli is also presented to the high-level control neuron. After STDP learning, the firing neurons are only those neurons that receive the same stimulus as the control neuron. STDP can increase the efficacy of these connections between neurons with synchronous signals, and decrease the weights of connections between neurons with asynchronous signals. The simulation results are shown in Fig. 7.10. This two-layers network can be used as a
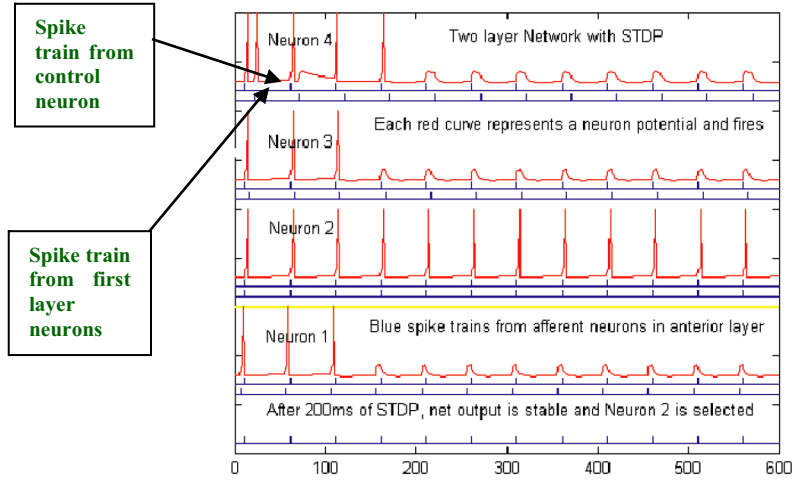
Figure 7.10.   Synchronized signals selected by STDP learning

spike train filter. It is capable of selecting the signal that is the same as that from the control neuron.

4.2   Non-linear Function Approximation

Let the input layer represent variable x and output layer represent variable y. By using the STDP learning mechanism, the two-layers network shown in Fig.7.11 can be trained to perform any non-linear function $y = f(x)$. At the training stage, a training stimulus is required to feed into the output layer. As shown in Fig.7.11, the training layer can generate the target stimulus according to $f(x)$ and feed into the output layer. A series of stimuli is randomly generated and presented to the input layer. At the same time the training layer applies the series of stimuli to generate target stimuli for the output layer. After STPD learning, the two-layer network can perform the function $y = f(x)$ without any training stimuli from the training layer i.e. after removal of the training stimuli.

For example, an SNN with three 100-neuron layers was trained to perform $y = \sin(x)$. The input layer is set to a circle chain with 100 neurons. The zero degree corresponds to Neuron 50. The output layer and training layer are set to 100 neurons respectively. If y is regarded as a one-dimensional co-ordinate, the origin of the y co-ordinate is set to Neuron 50. Let $y = 1$ correspond to Neuron 94. Because stimulus is a bell-shaped firing rate distribution, 6 neurons at the end of the neuron layer are used to deal with the stimulus. Similarly, let $y = -1$
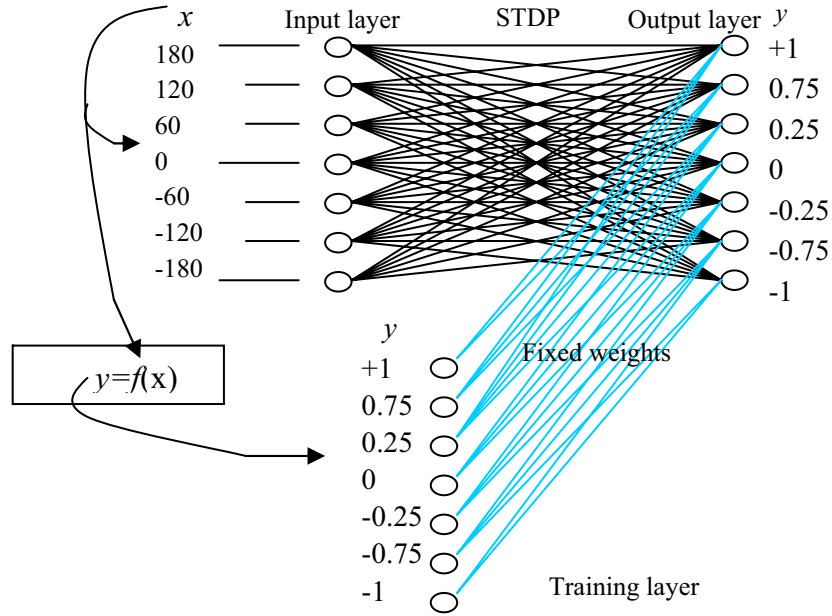
Figure 7.11. SNN trained with STDP for non-linear transformation

correspond to Neuron 6 instead of Neuron 1. If a stimulus is presented at x, the firing rate distribution of the bell-shaped stimulus is represented by following express.

$$f_x(x') = R_{\max}\mathrm{e}^{\frac{\cos\left(\frac{2\pi}{N}(x-x')\right)}{\delta^2}} \qquad (7.9)$$

where R_{max} is the maximal firing rate, N is the number of neurons in the layer, x' is the neuron numbers adjacent to the neuron at x position, and δ is a constant. If $x = 0$, the centre of stimulus is at Neuron 50. Note that not only Neuron 50 responds to the stimulus, but also those neurons adjacent to Neuron 50. This is very different from the values in classical neural networks or digital numbers in Turing computers. In order to easily generate the stimulus, the frequency can be transformed to Inter Spike Interval (ISI). ISI for each neuron in x layer can be represented as follows.

$$T_{isi}(x') = round(-\frac{1}{f_x(x')}\log(rand)) + 6 \qquad \text{(ms)} \qquad (7.10)$$

where x' is a neuron number adjacent to position x, and f is the firing rate of neuron x'. Note that a 6 ms refractory period is considered.
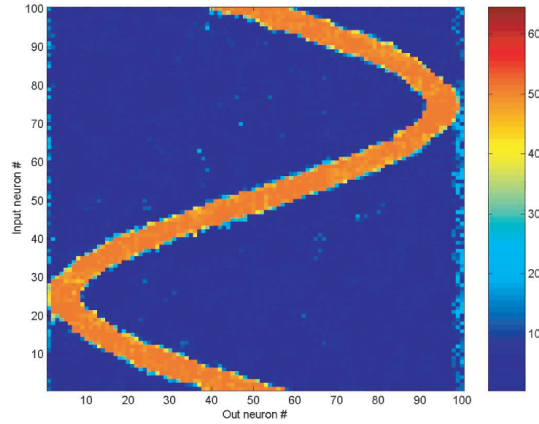
Figure 7.12.   Weight distribution for connections between input and output neurons

Stimuli for x and y are represented by stimuli that are firing rate distributions described using (7.9) and (7.10). The value of x is randomly chosen, and the value of y is calculated using the formula $y = \sin(x)$. This pair of x and y stimuli are presented to the input layer and training layer separately for 20 ms. The weight distribution is then updated by the STDP rule. After 20ms, a pair of x and y stimuli corresponding to another random x value is presented to the network for 20 ms. Repeating this procedure for 3000ms, the weight distribution converges to a stable distribution, as shown in Fig.7.12. The red point indicates the connection with the highest value of weight. With this weight distribution the two-layer network can perform the function $y = \sin(x)$. Example test results are shown in Fig. 7.13.

4.3   Stimuli Integration

A cue integration model was proposed in [25]. However, the STDP learning mechanism was not considered in the model. A similar SNN model with the STDP learning mechanism is proposed in Fig. 7.14. Three neuron layers x, y, z are connected to a 2D intermediate neuron layer. Suppose that neurons in the x and y layers are connected to neurons in x-RF and y-RF fields with excitatory synapses respectively, as shown by a solid line in Fig. 7.14. Neurons in the x and y layers are connected to neurons outside of the x-RF and y-RF fields with inhibitory synapses respectively, as shown by the short dash line in Fig.7.14. Neurons in the intermediate layer are fully connected to each neuron in the z neuron layer via STDP synapses, as shown by the long dash line in Fig. 7.14.
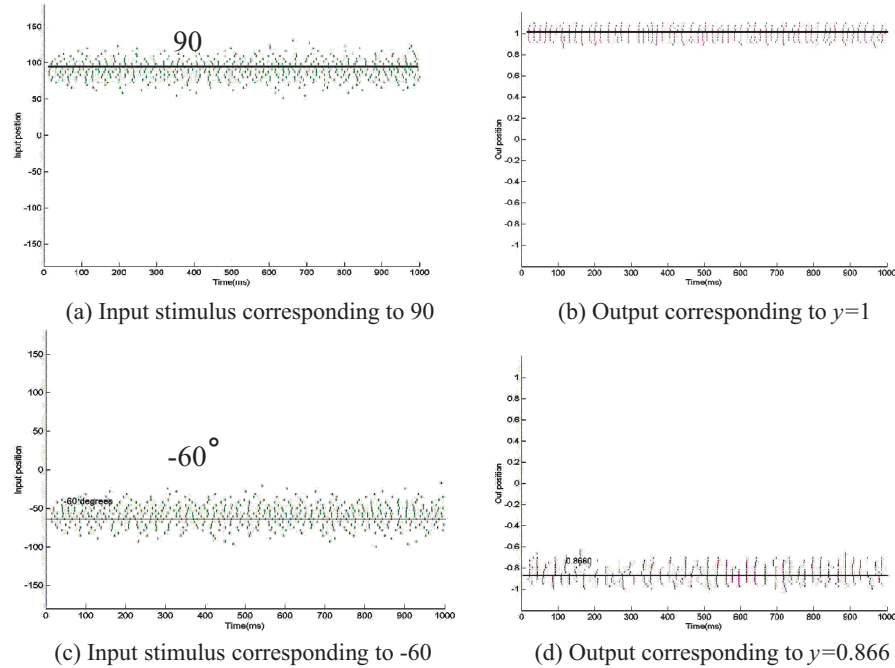
(a) Input stimulus corresponding to 90

(b) Output corresponding to $y=1$

(c) Input stimulus corresponding to -60

(d) Output corresponding to $y=0.866$

Figure 7.13.   Stimulus input and output neuron firing rate
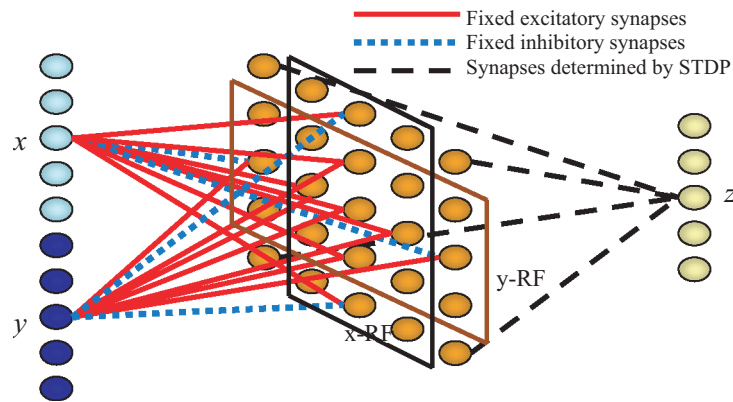
Figure 7.14.   Scratch for Architecture of Multiple Stimuli Integrating SNN.

When two stimuli are presented at the input neuron layers x and y, the target stimulus for $z = x + y$ is injected into z layer. The STDP synapses adapt to the stimuli. After training, the weights between the intermediate layer and the z layer are adapted to perform $z = x + y$. In the experiment, neuron layers x, y and z have 20 neurons respectively.
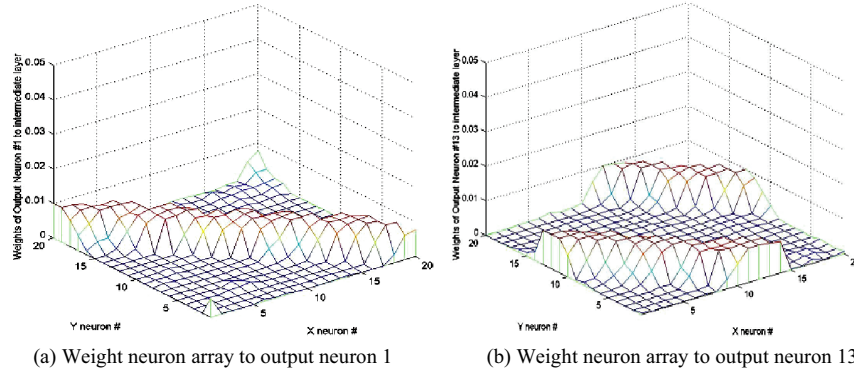
186   Q. Wu et al.

(a) Weight neuron array to output neuron 1   (b) Weight neuron array to output neuron 13

Figure 7.15.   Weight strength distribution for intermediate layer to z neuron layer.

(a)Two input stimuli, upper row for x, lower row for y (b)Output of z neuron layer
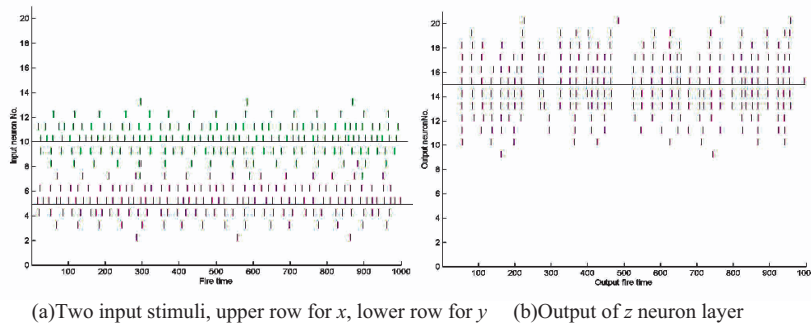
Figure 7.16.   Stimulus Test for $z = x + y$

The intermediate layer has $20 \times 20 = 400$ neurons. The weight distributions for Neuron 1 and Neuron 13 in the z layer are shown in Fig. 7.15. The test results are shown in Fig. 7.16.

5.   SNN Learning for XOR Problem

The traditional XOR problem and phase encoding scheme are applied to illustrate STDP learning paradigm in this section. In the phase encoding scheme spike trains are assumed in the same firing frequency. For different spike trains, the firing time is at a different phase. For example, suppose that the period is 10 ms and each phase corresponds to a time interval for 1 ms. Each period thus contains 10 phases. In order to indicate the periods, sine curves are plotted in Fig. 7.17. Phases also can be represented in radian or degree. Firing time at phase 7 stands for logical '0', and firing time at phase 2 stands for logical '1'. The logical '0' and '1' are represented by the spike trains (a) and (b) in Fig. 7.17. The

(a) Suppose that phase 7 (ph7) stands for logical '0'

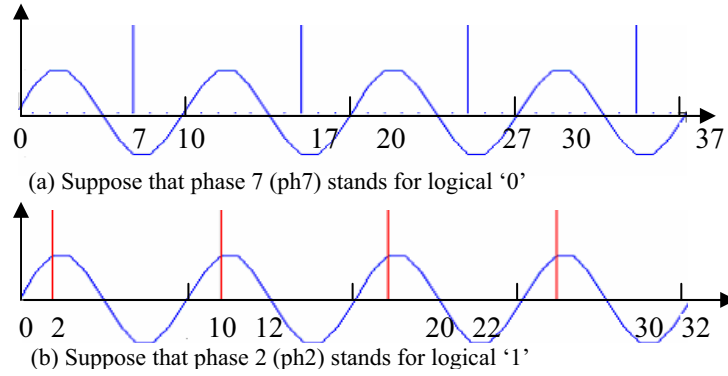(b) Suppose that phase 2 (ph2) stands for logical '1'

Figure 7.17. Phase encoding spike trains for logical '0' and '1'.
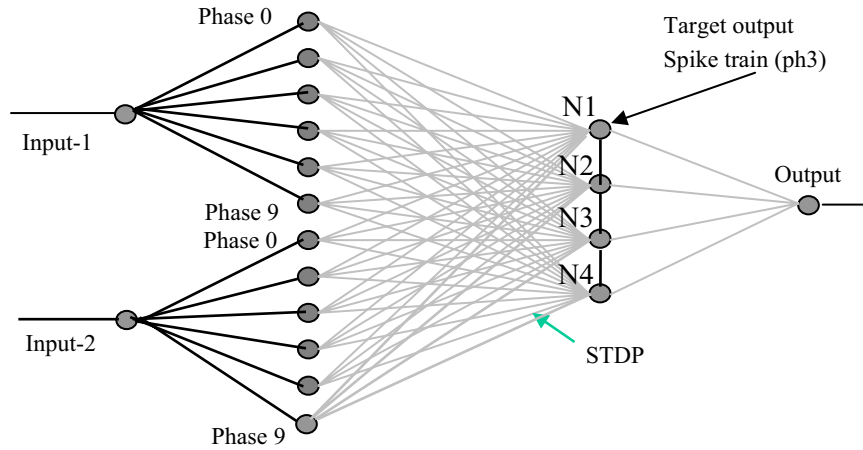
Figure 7.18. The spiking neural network for XOR problem

XOR problem can be represented as a set of training patterns shown in Table 7.2. As it takes time for the action potential to travel from delay neurons to neuron N1, N2, N3 and N4, the output spike at phase 3 represents logical '0', and output spike at phase 8 represents logical '1'. These patterns are applied to train the spiking neural network shown in Fig. 7.18.

Fig.7.18 shows the spiking neural network for the XOR problem. There are two inputs and one output in the network. Each input is connected to a set of neurons with a specific delay synapse. For example, input-1 is connected to a Phase 0 neuron without any delay, and it is connected to a Phase 1 neuron with a delay 1 ms, Phase 2 neuron with a delay 2 ms, ..., Phase 9 neuron with a delay 9 ms. Similarly, input-2

Table 7.2.   Training patterns associations for XOR problem

| Pattern No.	Input-1	Input-2	Output
1	1-(ph7)	1-(ph7)	0-(ph3)
2	1-(ph7)	0-(ph2)	1-(ph8)
3	0-(ph2)	1-(ph7)	1-(ph8)
4	0-(ph2)	0-(ph2)	0-(ph3)

is also connected to 10 delay neurons. Therefore, two temporal phase encoding spike trains are transferred to activities of delay neurons, i.e. spatial-encoding patterns.

N1, N2, N3, and N4 are four pattern recognition neurons that are fully connected to all delay neurons with STDP synapses. These connections ensure that the network can adapt to the training patterns by the STDP rule. Four pattern recognition neurons are connected to each other with inhibitory synapses. These inhibitory synapses make a competition mechanism among the four pattern recognition neurons. Once a neuron fires, the neuron will inhibit other neurons firing. This makes it possible for one neuron to respond to one stable input pattern. There are four patterns in the XOR problem. Four neurons are employed in this layer.

If one wants to train the network to recognize XOR pattern 1 in Table 7.2, the phase encoding spike train (b) is fed into input-1 and input-2. At the same time, the target output spike train (ph8) is injected into neuron N1. After about 150ms for STDP adaptation, the connection weights from N1 to all delay neurons converge to a stable distribution, and the neuron N1 can respond to the input pattern. Similarly, neuron N2, N3, and N4 can be trained to recognize pattern 2, 3, and 4. After this, the network can perform the XOR function. The test results are shown in Fig. 7.19.

6.   SNN Learning for Coordinate Transformation

The brain receives multiple sensory data from the surrounding environments where the different senses do not operate independently, but there are strong links between modalities [26], [27]. Electrophysiological studies have shown that the somatosensory cortex (SI) neurons in monkeys respond not only to touch stimulus but also to other modalities. Strong links between vision and touch have been found in behavioural [28] and electrophysiological [29] studies, and at the level of single neurons [30]. For example, neurons in the somatosensory cortex (SI) may respond to visual stimuli [31] and other modalities [32]. Neurons in a
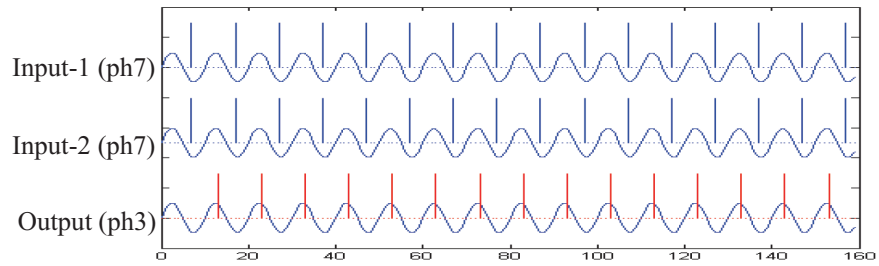
(a) Test results for pattern 1
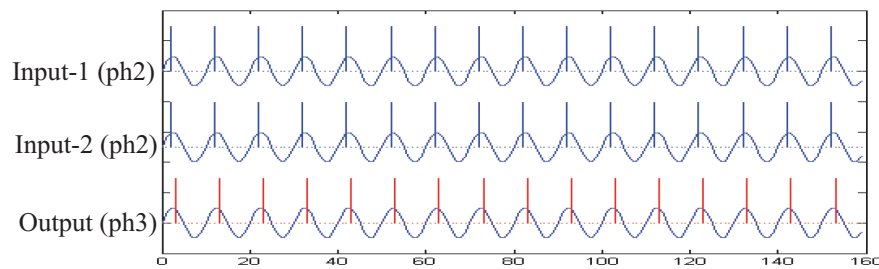
(b) Test results for pattern 2
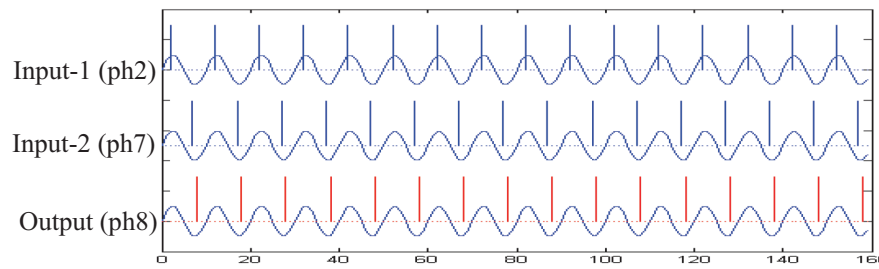
(c) Test results for pattern 3

(d) Test results for pattern 4

Figure 7.19.   Test results of the spiking neural network for XOR problem

monkey's primary SI may fire both in response to a tactile stimulus and also in response to a visual stimulus [31].

A new interaction between vision and touch in human perception is proposed in [33]. These perceptions may particularly interact during fine manipulation tasks using the fingers under visual and sensory control [34]. Different sensors convey spati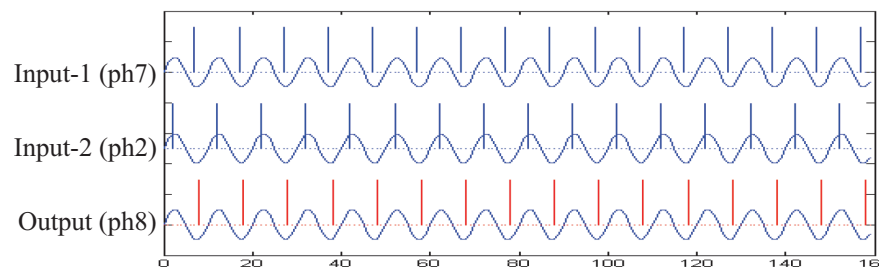al information to the brain with different spatial coordinate frames. In order to plan accurate motor actions, the brain needs to build an integrated spatial representation. Therefore, cross-modal sensory integration and sensory-motor coordinate transformations must occur [35]. Multimodal neurons using non-retinal bodycentred reference frames are found in the posterior parietal and frontal cortices of monkeys [36], [37], [38]. Basis function networks with multidimensional attractors [25] are proposed to simulate the cue integration and co-ordinate transformation properties that are observed in several multimodal cortical areas. Adaptive regulation of synaptic strengths within SI could explain modulation of touch by both vision [39] and attention [40]. Learned associations between visual and tactile stimuli may influence bimodal neurons.

Based on these concepts, a spiking neural network (SNN) model [42] is proposed to perform the co-ordinate transformation required to convert a time-coded haptic input to a space-coded visual image. The SNN model contains STDP synapses from haptic intermediate neurons to the bimodal neurons.

In order to simulate location related neurons in the somatosensory cortex (SI), suppose that X and Y are single layers of bimodal neurons that represent the Cartesian co-ordinates of the output. Fig. 7.20 shows a simplified SNN model for building associations between visual and haptic stimuli.

If the eyes focus on a point (x, y) at the touch area, a visual stimulus can be generated and transferred to the X and Y bimodal neuron layers through the visual pathway. Therefore, the visual signal can be applied to train the SNN for the haptic pathway. If a finger touches the point (x, y), a haptic stimulus will trigger (θ, Φ) stimuli corresponding to arm position. The (θ, Φ) stimuli are transferred to (X, Y) bimodal neuron layers through the haptic pathway. In this model, the synapse strength for the visual pathway is assumed to be fixed values. Each neuron in the X layer is connected to retinal neurons with a vertical line receptive field shown in Fig. 7-20. Each neuron in Y layer is connected to retinal neurons with a horizontal line receptive field. In this experiments, R_{max} for bell shaped stimuli is set to 80/s, and δ is set to 0.04, and 40 neurons are employed to encode the θ and Φ layers respectively. 1600 neurons are employed in the 2D intermediate layer and 80 neurons in the
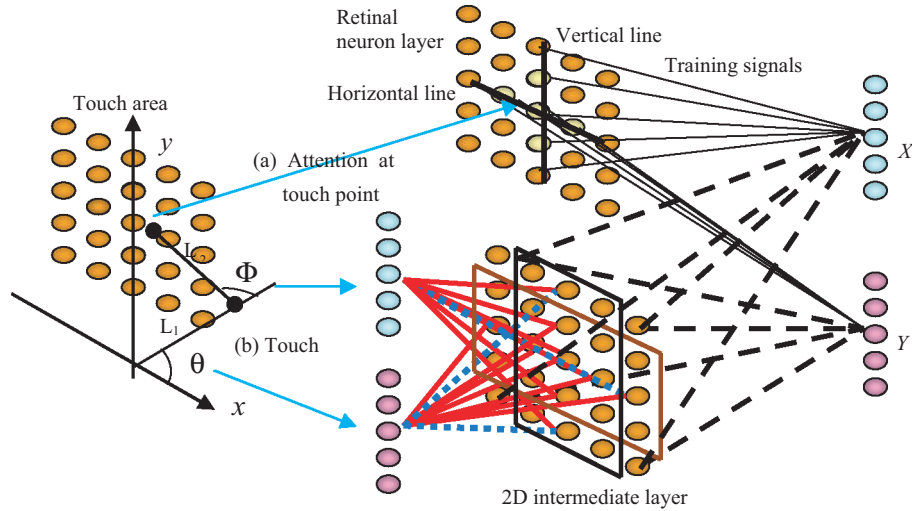
Figure 7.20. A SNN model for 2D co-ordinate transformation. (x, y) is co-ordinate for touch area. (a) Visual pathway: the retinal neuron layer is represented by 2D layer with 40X40 neurons that are connected to X and Y neuron layer with fixed weights. (b) Haptic pathway: L_1 and L_2 are arms. θ and Φ are arm angles represented by a 1D neuron layer respectively. Each θ neuron is connected to the neurons within a corresponding vertical rectangle in the 2D intermediate layer. Each Φ neuron is connected to the neurons within a corresponding horizontal rectangle in the 2D intermediate layer. The neurons in the intermediate layer are fully connected to the X and Y neuron layers with STDP synapses. These connections are adapted in response to the attention visual stimulus and haptic stimulus under STDP rules.

training layer respectively. 80 neurons are also employed in the X and Y layers respectively.

After training, the SNN can transform the (θ, Φ) stimuli to output (X, Y) neuron spike activities. In order to test the SNN, suppose that the forearm turns around with a speed $40°$ per second, as shown in Fig. 7.21. The circle is the track of the finger. The values of (θ, Φ) are applied to generate Poisson procedure spike trains for θ and Φ layers according to (7.9) and (7.10). When the finger traces the circumference following the track of the circle, two stimuli are generated corresponding to (θ, Φ) of the arm. The stimuli are shown in the left panel in Fig. 7.22. When the two stimuli are input into the network, the outputs of the (X, Y) neuron layers obtained are displayed in the right panel of Fig.7.22. The neuron firing-rate at the output layer is a bell-shape distribution. Transferring these firing rate to single values of X and Y, we can demonstrate that
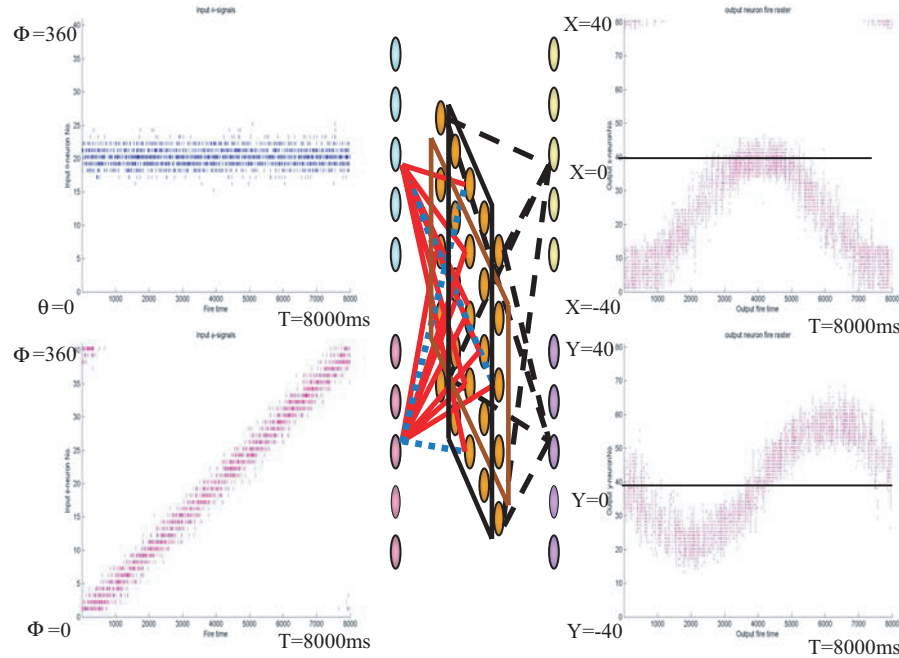
Figure 7.21.   The track of finger movement

the SNN is capable of transferring the polar co-ordinate (θ, Φ) to the Cartesian representation (X, Y) as in the equations.

$$X = L[\cos(\theta) + \cos(\theta + \Phi)] \qquad (7.11)$$
$$Y = L[\sin(\theta) + \sin(\theta + \Phi)] \qquad (7.12)$$

The spike train raster in the upper-left panel in Fig.7.22 represents the stimuli corresponding to $\theta = 180°$. The stimuli persists for 8000ms. The stimuli for the Φ neuron layer is shown in the lower-left panel. The stimuli with bell-shaped firing rate distribution stays for 200ms in sequent positions at $\Phi = 0°, 9°, 18°, \ldots 360°$. The changes of (θ, Φ) correspond to the finger moving along a circle with radius L. According to (7.11) and (7.12), the output $X = L(-1 - \cos(\Phi))$ and $Y = -L\sin(\Phi)$. These mathematical results are consistent with the SNN outputs shown in the right panel.

The results of learning are stored in the weight distribution of the connections between the 2D intermediate layer and (X, Y) layers. After learning, the haptic pathway in the SNN can transform the arm position (θ, Φ) to (X, Y) bimodal neuron layers. Actually, θ and Φ are based on body-centred co-ordinates, which are polar co-ordinates. The neurons in θ and Φ layers transfer haptic location signals to the intermediate

Figure 7.22.   Co-ordinate transformation from body-centred co-ordinate (θ, Φ) to (X, Y).

layer, and then this intermediate layer transfers the body-centred co-ordinate to the integrated co-ordinate X and Y neuron layers. The STDP synapses make it possible to learn and transform body-centred co-ordinate (θ, Φ) to co-ordinate (X, Y). The co-ordinate (X, Y) can be regarded as integrated co-ordinates in the brain. In this situation, co-ordinate (X, Y) is actually the retina-centred co-ordinate. The transformation is equivalent to transformation from a haptic body-centred co-ordinate to a retina-centred co-ordinate.

7.   Conclusion

In this chapter, a number of spiking neuron models were mentioned, and the conductance-based integrate-and-fire neuron model was introduced in detail. All the demonstrations are based on this model. As spiking neurons transfer information via spike trains, the neuron encoding scheme plays a very important role in learning mechanisms. In this chapter, a circle of neuron chain was applied to represent an angular variable. A neuron chain was applied to represent a single variable.

Based on these representations, SNNs were trained to perform non-linear function approximation, and cue integration z = x + y.

By using phase encoding scheme, a solution of the XOR problem was demonstrated. All the learning mechanisms demonstrated here are based on STDP. These demonstrations only give simple examples so as to assist in understanding STDP. Based on these principles, more complicated SNNs can be simulated in a further study.

In a biological system, there are strong links between modalities. A cross modality learning model for co-ordinate transformation was proposed. In the SNN model, the network was trained to perform co-ordinate transformation from the arm angles of the haptic stimuli position to a position represented by retina-centred co-ordinate.

The advantage of spiking neural networks is that they are more robust and provides better noise immunity than classical neural networks, even if some of the neurons do not work. The learning mechanisms can provide an approach for designing artificial intelligent systems to process biological stimuli.

Acknowledgement

References

[1] Maass, W., Schnitger, G., and Songtag, E.: On the computational power of sigmoid versus Boolean threshold circuits. Proc. of the 32nd Annual IEEE Symposium on Foundations of Computer Science. (1991)767–776

[2] Maass, W.: Networks of spiking neurons: The third generation of neural network models. Neural Networks. 10(9): (1997)1659–1671

[3] Hodgkin, A. and Huxley, A.: A quantitative description of membrane current and its application to conduction and excitation in nerve. Journal of Physiology. (London) Vol. 117, (1952)500–544

[4] Gerstner, W., and Kistler, W.: Spiking Neuron Models. Single Neurons, Populations, Plasticity. Cambridge University Press, (2002)

[5] Melamed, O., Gerstner, W., Maass, W., Tsodyks, M. and Markram, H.: Coding and Learning of behavioral sequences, Trends in Neurosciences, Vol. 27 (2004)11–14

[6] Theunissen, F.E. and Miller, J.P.: Temporal Encoding in Nervous Systems: A Rigorous Definition. Journal of Computational Neuroscience. (1995)2: 149–162

[7] Bohte, S.M., Kok, J.N. and Poutré, H.L.: SpikeProp: Error-Backpropagation for Networks of Spiking Neurons. Neurocomputing. 48(1–4) (2002)17–37

[8] Wu, Q.X., McGinnity, T.M., Maguire L.P., Glackin, B. and Belatreche, A.: Supervised Training of Spiking Neural Networks With Weight Limitation Constraints. Proceedings of International conference on Brain Inspired Cognitive Systems. University of Stirling, Scotland, UK, (2004)

[9] Sohn, J.W., Zhang, B.T., and Kaang, B.K.: Temporal Pattern Recognition Using a Spiking Neural Network with Delays. Proceedings of the International Joint Conference on Neural Networks (IJCNN'99). vol. 4 (1999)2590–2593

[10] Lysetskiy, M., Ozowski, A., and Zurada, J.M.: Invariant Recognition of Spatio-Temporal Patterns in The Olfactory System Model, Neural Processing Letters. 15:225–234, Kluwer Academic Publishers. Printed in the Netherlands, 2002

[11] Choe, Y. and Miikulainen, R.: Self-organization and segmentation in a laterally connected orientation map of spiking neurons. Neurocomputing. 21 (1998)139–157

[12] Sirosh, J., and Miikkulainen, R.: Topographic receptive fields and patterned lateral interaction in a selforganizing model of the primary visual cortex. Neural Computation. 9 (1997) 577–594

[13] Bi, G.Q., and Poo, M.M.: Distributed synaptic modification in neural networks induced by patterned stimulation. Nature, 401 (1999)792–796

[14] Bi, G.Q., Poo, M.M.: Synaptic modifications in cultured hippocampal neurons: dependence on spike timing, synaptic strength, and postsynaptic cell type. Journal of Neuroscience. 18 (1998)10464–10472

[15] Bell, C.C., Han, V.Z., Sugavara, Y., and Grant, K.: Synaptic plasticity in the mormyrid electrosensory lobe. Journal of Experimental Biology. 202 (1999)1339–1347

[16] Rossum, M.C.W., Bi, G.Q., and Turrigiano, G.G.: Stable Hebbian Learning from Spike Timing-Dependent Plasticity. The Journal of Neuroscience. 20(23)(2000)8812–8821

[17] Neuron Software download website: http://neuron.duke.edu/

[18] Wu, Q.X., McGinnity, T.M., Maguire, L.P., Glackin, B. and Belatreche, A.: Learning under weight constraints in networks of temporal encoding spiking neurons. International Journal of Neurocomputing. Special issue on Brain Inspired Cognitive Systems. (2006) in press.

[19] Müller, E.: Simulation of High-Conductance States in Cortical Neural Networks. Masters thesis, University of Heidelberg, HD-KIP-03-22, (2003)

[20] Koch, C.: Biophysics of Computation: Information Processing in Single Neurons. Oxford University Press, (1999)

[21] Dayan, P., and Abbott, L.F.: Theoretical Neuroscience: Computational and Mathematical Modeling of Neural Systems. The MIT Press, Cambridge, Massachusetts, (2001).

[22] SenseMaker Project (IST–2001-34712) funded by the European Union under the "Information Society Technologies" Programme (2002-2006)

[23] Song, S., Miller, K.D., and Abbott, L.F.: Competitive Hebbian learning though spike-timing dependent synaptic plasticity. Nature Neuroscience, 3 (2000) 919–926

[24] Song, S., and Abbott, L.F.: Column and Map Development and Cortical Re-Mapping Through Spike-Timing Dependent Plasticity. Neuron, 32 (2001) 339–350

[25] Deneve S., Latham P. E. and Pouget A.: Efficient computation and cue integration with noisy population codes, Nature Neuroscience, 4 (2001) 826–831

[26] Marisa T.C., Kennett, S., and Haggard, P.: Persistence of visual-tactile enhancement in humans. Neuroscience Letters. Elsevier Science Ltd, 354(1)(2004) 22–25

[27] Atkins, J. E., Jacobs, R.A., and Knill, D.C.: Experience-dependent visual cue recalibration based on discrepancies between visual and haptic percepts. Vision Research. 43(25) (2003) 2603–2613

[28] Spence, C., Pavani, F., and Driver, J.: Crossmodal links between vision and touch in covert endogenous spatial attention. Journal of Experimental Psychology: Human Perception and Performance. 26 (2000) 1298–1319

[29] Eimer M., Driver, J.: An event-related brain potential study of crossmodal links in spatial attention between vision and touch. Psychophysiology. 37 (2000) 697–705

[30] Graziano, M.S.A., and Gross, C.G.: The representation of extrapersonal space: A possible role for bimodal, visual–tactile

neurons, in: M.S. Gazzaniga (Ed.), The Cognitive Neurosciences, MIT Press, Cambridge, MA, (1994) 1021–1034

[31] Zhou, Y.D., and Fuster, J.M.: Visuo-tactile cross-modal associations in cortical somatosensory cells. Proc. National Academy of Sciences, USA. 97 (2000) 9777–9782

[32] Meftah, E.M., and Shenasa, J.: Chapman, C.E., Effects of a cross-modal manipulation of attention on somatosensory cortical neuronal responses to tactile stimuli in the monkey. Journal of Neurophysiology. 88 (2002) 3133–3149

[33] Kennett, S., Taylor-Clarke, M., and Haggard, P.: Noninformative vision improves the spatial resolution of touch in humans. Current Biology. 11 (2001) 1188–1191

[34] Johansson, R.S., and Westling, G.: Signals in tactile afferents from the fingers eliciting adaptive motor-responses during precision grip. Experimental Brain Research. 66 (1987) 141–154

[35] Galati, G., Committeri, G., Sanes J.N., and Pizzamiglio L.: Spatial coding of visual and somatic sensory information in body-centred coordinates. European Journal of Neuroscience. Blackwell Publishing. 14(4) (2001) 737–748

[36] Colby, C.L. and Goldberg, M.E.: Space and attention in parietal cortex. Annual Review of Neuroscience. 22 (1999) 319–349

[37] Gross, C.G., and Graziano, M.S.A.: Multiple representations of space in the brain. Neuroscientist, 1 (1995) 43–50

[38] Rizzolatti, G., Fogassi, L. and Gallese, V.: Parietal cortex: from sight to action. Current Opinion in Neurobiology. 7 (1997) 562–567

[39] Taylor-Clarke M., Kennett S., and Haggard P.: Vision modulates somatosensory cortical processing. Current Biology. 12 (2002) 233–236

[40] Iriki, A., Tanaka, M., and Iwamura, Y.: Attention-induced neuronal activity in the monkey somatosensory cortex revealed by pupillometrics. Neuroscience Research. 25 (1996) 173–181

[41] Thorpe, S., Delorme A. and Rullen, R.V.: Spike-based strategies for rapid processing. Neural Networks.14(6–7) (2001)715–725

[42] Wu, Q.X., McGinnity, T.M., Maguire, L.P., Belatreche, A. and Glackin, B.: Adaptive Co-Ordinate Transformation Based on Spike Timing-Dependent Plasticity Learning Paradigm. Proceedings of The First International Conference on Natural Computation, LNCS, 3610 (2005)420–429